Electronic Supplementary Material (ESI) for Journal of Materials Chemistry A.

Ion-Terminated Hyperbranched Polymer Towards Multipurpose Adhesive with Record-High Bonding Strength and Sensitive Stress-Sensing

Haiming Chen[1], Haohao Lin[1,2], Zaizheng Sun[1], He Li[1], Chaobin He[3,4], Dongsheng Mao[1]**

1. Key Laboratory of Marine Materials and Related Technologies, Zhejiang Key Laboratory of Marine Materials and Protective Technologies, Ningbo Institute of Materials Technology and Engineering, Chinese Academy of Sciences, Ningbo, 315201, China
2. Faculty of Electrical Engineering and Computer Science, Ningbo University, Ningbo 315211, China.
3. Department of Materials Science and Engineering, National University of Singapore, Singapore, 117575 Singapore
4. Institute of Materials Research and Engineering, Singapore, 138634 Singapore

Corresponding author (*):

Dongsheng Mao Email address: maodongsheng@nimte.ac.cn

Chaobin He Email address: msehc@nus.edu.sg

Materials and experimental

Materials:

Poly(propylene glycol) bis(2-aminopropyl ether) (polyetheramine) with molecular weight of 230 (D230) and 400 (D400), 1,6-hexylenediamine (HDA), N,N-methylene-bis-acrylamide (MBA), methacrylatoethyl trimethyl ammonium chloride (MTAC), Lithium bis(trifluoromethanesulphonyl) imide (LiTFSI), were purchased from Aladdin (Shanghai, China). Methanol was purchased from J&K scientific. All reagents were commercially available and used as supplied without further purification.

Experimental

Synthesis of hyperbranched polymers

The randomly hyperbranched polymers were synthesized by Michael addition reaction between D230/MBA, D400/MBA or HAD/MBA with various molar ratios. In all specimens, the molar ratio of primary amine group was set as 1.0 and the molar ratio of MBA varied from 0.8 to 1.0, thus the materials were denoted as D230-x, D400-x and HDA-x, where x corresponds to MBA molar ratios of 0.8, 0.9 and 1.0 respectively. For example, in a typical procedure, the synthesis of D230-0.9 was described as follows:

Step 1: MBA (6.93 g, 0.045 mol) was added into a round bottom flask equipped with a magnetic stirrer containing mixed solvent of 45 mL methanol and 22.5 mL deionized water at 30 °C and stirred until it was dissolved totally. Then D230 (11.5 g, 0.05 mol) was fed into the flask directly. The mixture was stirred at 60 °C for 24 h.

Step 2: MTAC (18.72 g, 0.09 mol) was added into above solution and continue stirred at 60 °C for 24 h. Here the amount of MTAC was depended on the residual amounts of amine group in step 1 in order to consume all amines.

Step 3: Excess LiTFSI aqueous solution (with concentration of 37.5%) was added into above solution and continue stirring until a precipitate settles out. Then the crude product was washed 5 times with deionized water to obtain a solid and then dried in a vacuum oven at 70 °C for 12 h.

The schematic diagram of synthetic reaction mechanism and the synthetic route of such hyperbranched polymers were shown in **Figure S1** and **S2**, respectively. The -NH- of D230, D400

and HDA can react with a CH_2=CH- on MBA and MTAC under a mild condition to fabricate hyperbranched polymeric molecules. And the reaction can form new secondary amines and tertiary amines.

Preparation of adhesion layers:

PSA: The adhesives was covered on the surface of the substrate, then a surface was covered on the adhesive layer at room temperature. After that the adhesion area was pressed by a dovetail clip for 60 min. Then a thin coating layer was formed and two surfaces were adhered firmly. The adhered surface pairs can be directly used for different tests without any further operation.

HMA: The adhesives were covered on the surface of the substrate, then a surface was covered on the adhesive layer at 160 °C. After that the adhesion area was pressed by a dovetail clip and cooling to room temperature. The pressed time by a dovetail clip is 60 min. Then a thin coating layer was formed and two surfaces were adhered firmly. The adhered surface pairs can be directly used for different tests without any further operation.

Characterisation

The chemical structure were characterized by a FTIR (Nicolet 6700, Thermo Scientific), operating in transmission mode from sample films cast onto KBr disks. The calculation process of total content of H-bonds and the content of order H-bonds is expressed as: the total content of H-bonds = $1-\frac{A_{Free}}{A_{total}}\times 100\%$, and the content of order H-bonds = $\frac{A_{order}}{A_{total}}\times 100\%$. ^{1}H Nuclear Magnetic Resonance (^{1}H-NMR) spectra were measured by AVANCE III 400MHz spectrometer using $CDCl_3$ as a solvent at room temperature. Thermogravimetric Analyzer (TGA) experiments were carried out with a TA instruments' TGA209F1 with a heating rate of 20 °C/min from 50 to 700 °C. Differential scanning calorimetry (DSC) was carried out with NETZSCH DSC214, a cyclic heating/cooling run programme was taken under the rate of 10 °C/min at the temperature of -100 to 160 °C. Energy dispersive X-ray (EDX) spectra were collected on a Regulus-8230 scanning electron microscopy. Mechanical properties conducted at room temperature by using an MTS (2 kN) tensile machine. Five specimens of each composition were tested, the data reported were the average values. The

specimens used as adhesives for lap-shear tests were conducted in an open environment with a humidity of 50-60%. The self-healing efficiency was calculated based on toughness, elongation at break and strength is $\frac{W_{sh}}{W}\times 100\%$, $\frac{\varepsilon_{b-sh}}{\varepsilon_b}\times 100\%$, and $\frac{T_{sh}}{T}\times 100\%$, respectively, where the W_{sh} and W are the energy consumed during stretching of self-healed specimen and prisine specimen respectively, $\varepsilon_{b\text{-}sh}$ and ε are the elongation at break of self-healed specimen and prisine specimen respectively, T_{sh} and T are the stretching strength of self-healed specimen and prisine specimen respectively. The resistance change were collected by electrometer (Keithley 6514). Rheological properties were performed on an oscillatory rheometer (Discovery HR-3, TA) using a 25 mm parallel plate-plate geometry. Prior to each experiment, approximately 1.2 mm thick film samples were prepared, and each film sample was placed between the parallel plates. A temperature-sweep experiment was carried out between 25 and 160 °C at an ω and shear strain of 1 rad/s and 1%, respectively. In addition, frequency sweeping was carried out at each temperature in the 0.05−500 rad/s ω range at a constant shear strain of 1%. To establish a time-temperature superposition (TTS) master curve, data were acquired at intervals of 20 °C in the 30-110 °C range. TTS master curves of G' and G" were constructed from the frequency-sweep data by shifting the data to the reference temperature (25 °C).

Supplementary tables and figures

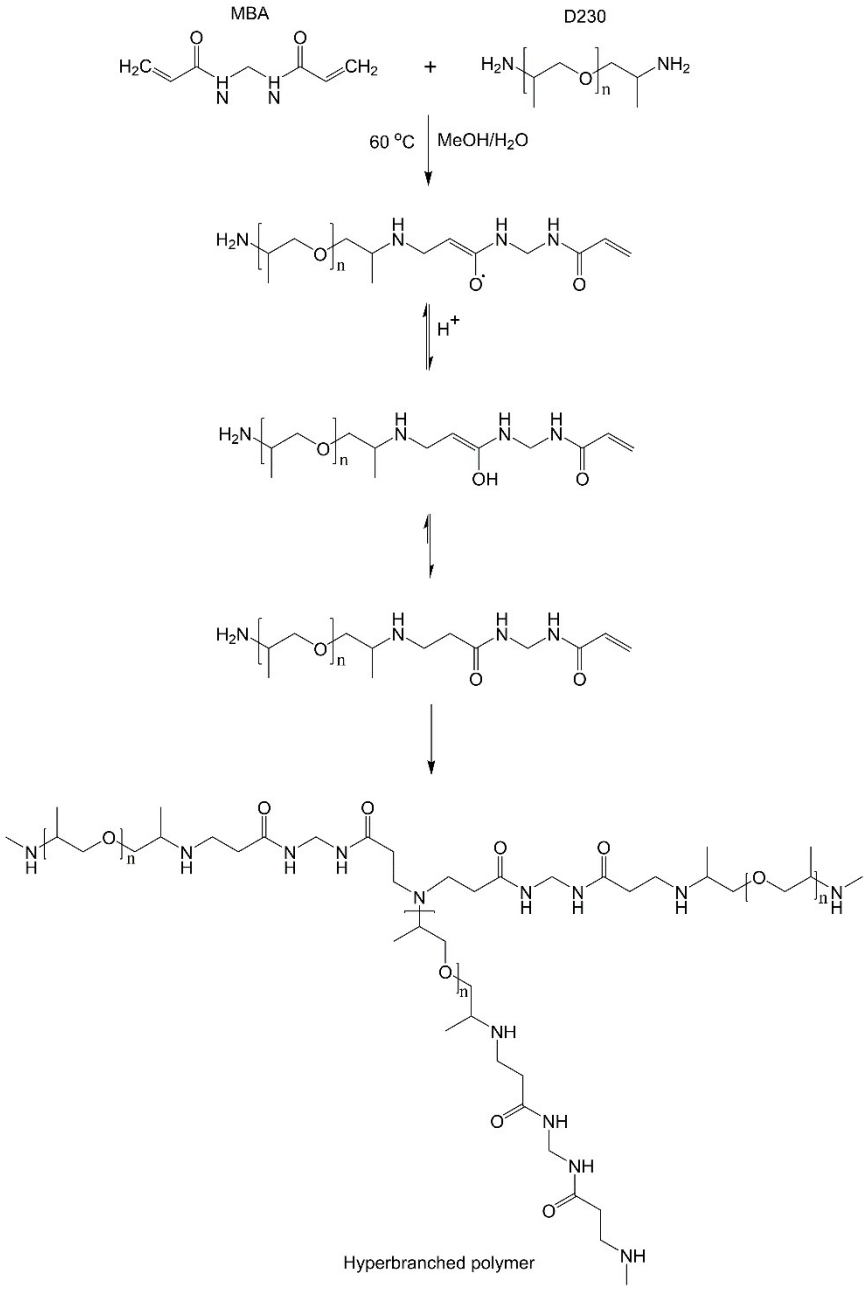

Figure S1. The schematic diagram of synthetic reaction mechanism of the hyperbranched polymers. The -NH- of D230, D400 and HDA can react with a CH_2=CH- on MBA and MTAC under a mild condition to fabricate hyperbranched polymeric molecules. And the reaction can form new secondary amines and tertiary amines.

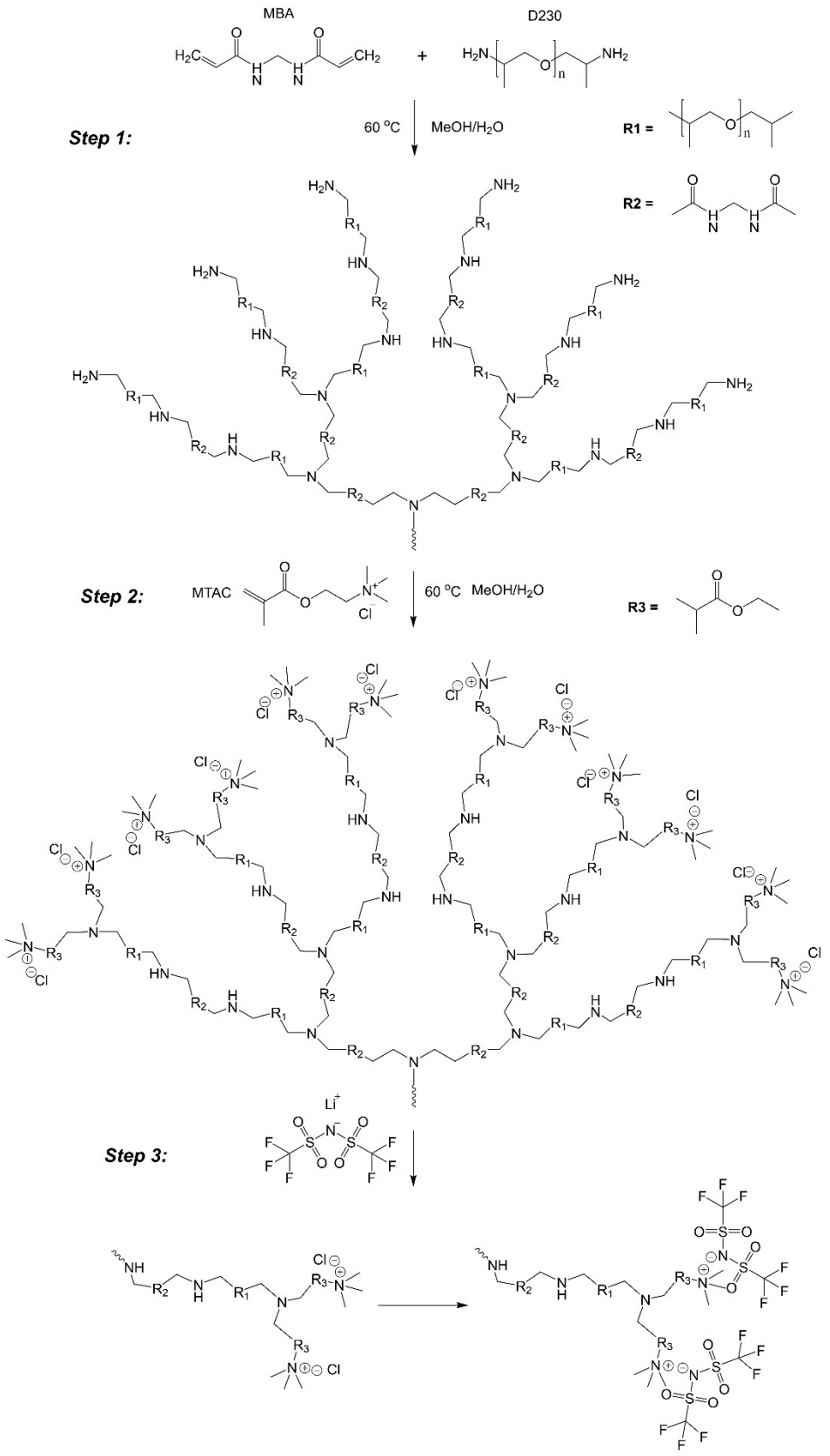

Figure S2. The synthetic route of the D230-0.9. The synthetic route of other specimens are similar with the one of D230-0.9 so those are omitted here.

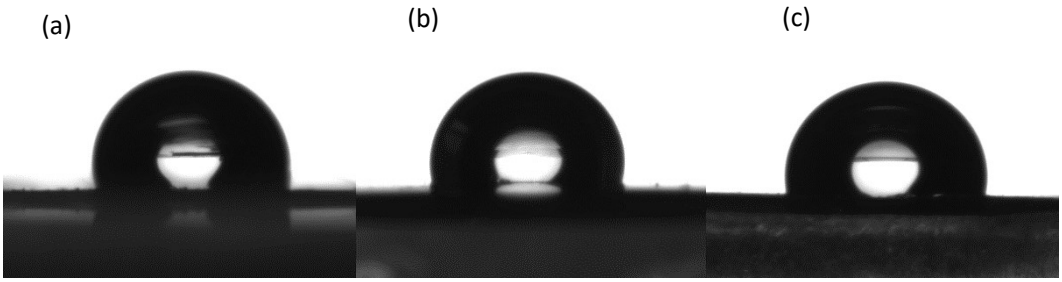

Figure S3. The D230-0.8, D230-0.9 and D230-1.0 show a water contant angle of 107.3° (a), 106.6°(b) and 106.5°(c), respectively.

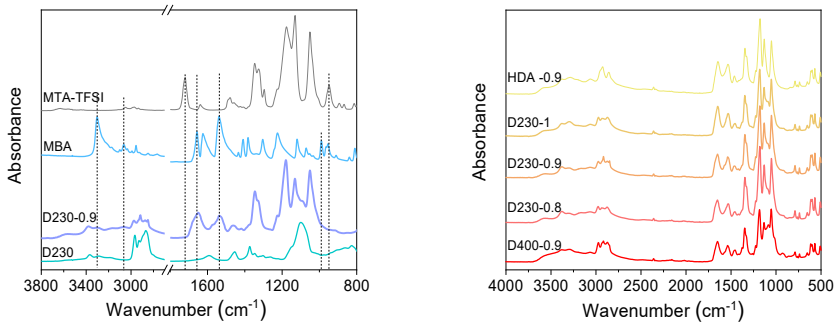

Figure S4. FTIR spectra of methacrylatoethyl trimethyl ammonium bis(trifluoromethanesulphonyl) imide (MTA-TFSI), MBA, D230, and D230-0.9, respectively. In the FTIR spectrum of MBA, the characteristic peaks at 3302 cm^{-1}, 1656 cm^{-1}, 1538 cm^{-1} are belonged to the strong stretching vibration of N-H group, C=O stretching vibration peak and N-H bending vibration peak, respectively, while the peaks at 987 cm^{-1} and 950 cm^{-1} are assigned to the bending vibration peaks of vinyl groups [1]. In D230-0.9, the characteristic amide I band at around 1650 cm^{-1}, amide II band at around 1537 cm^{-1} and disappeared vinyl group bending vibration peak indicate that the Michael addition reaction consumes all double bonds and hyperbranched networks are successfully formed. Here, the MTA-TFSI is the precipitate from the mixed aqueous solution of both LiTFSI and MTAC, which is an ionic liquid with hydrophobic properties.

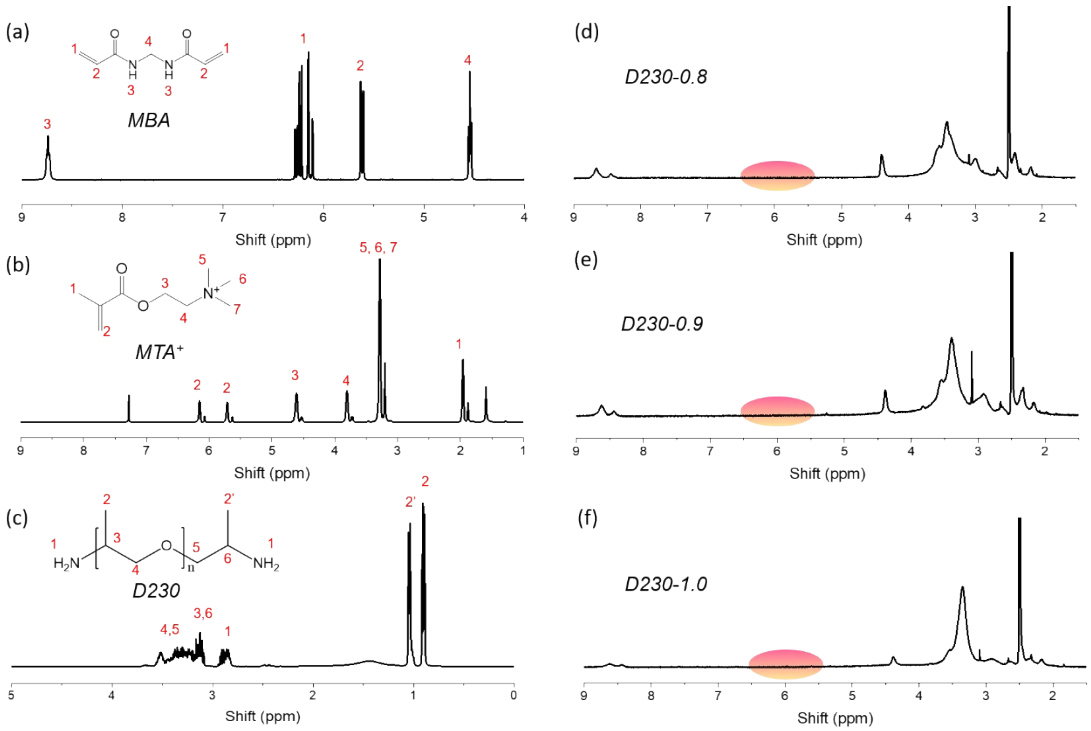

Figure S5. ^{1}H-NMR spectra of (a) MBA, (b) MTAC, (c) D230 chemicals and the synthesized hyperbranched polymer of (d) D230-0.8, (e) D230-0.9, (f) D230-1.0, respectively. The typical proton signals at 6.25 ppm and 5.70 ppm corresponding to vinyl groups disappear after reaction, while new signals appear at 2-3 ppm belonging to the methylene of -CH_2-CH_2-CONH-. It indicates that all the vinyl groups have been consumed.[2]

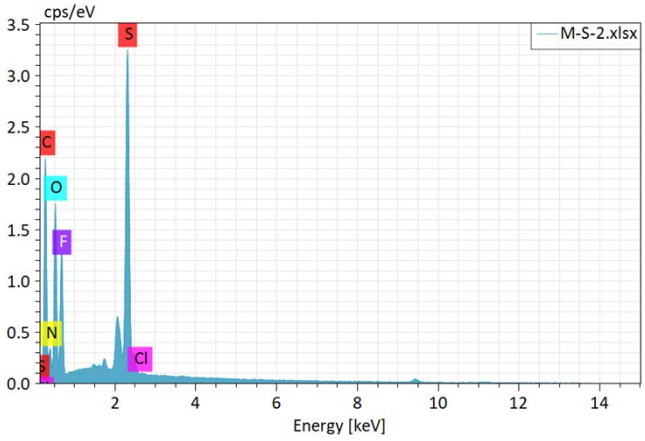

Figure S6. The energy dispersive X-ray spectroscopy of D230-0.8.

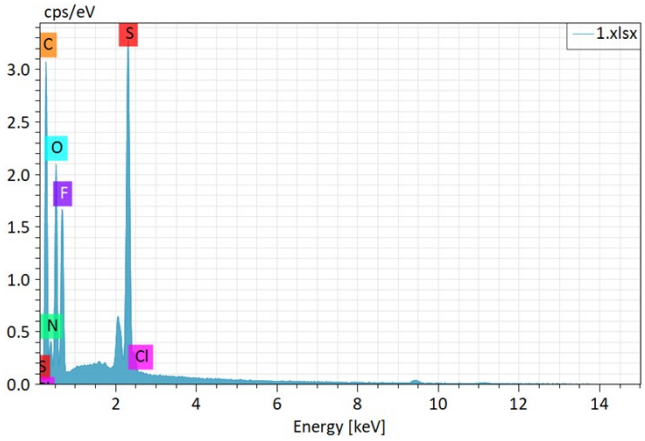

Figure S7. The energy dispersive X-ray spectroscopy of D230-0.9.

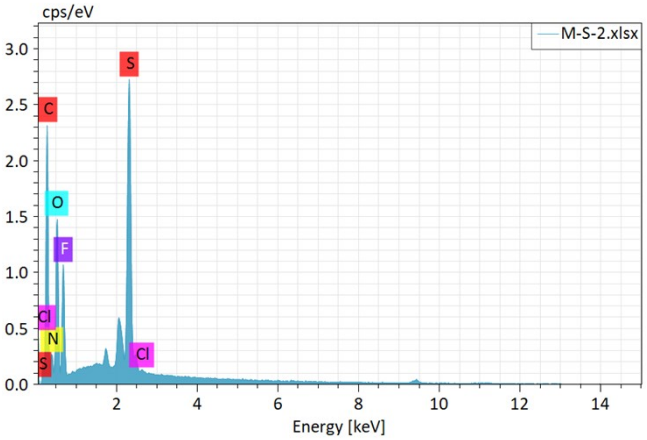

Figure S8. The energy dispersive X-ray spectroscopy of D230-1.0.

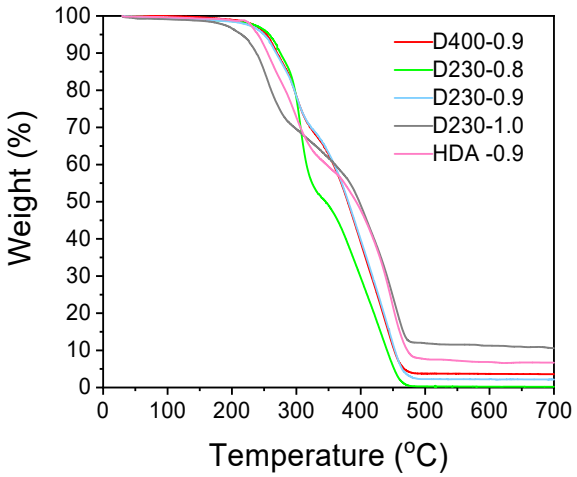

Figure S9. The TGA curves of such hyperbranched polymers.

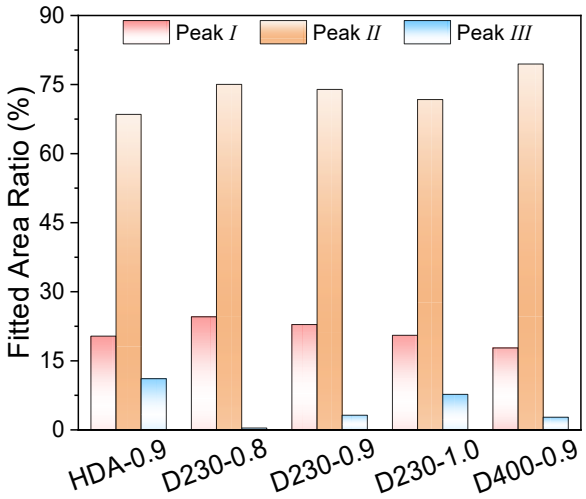

Figure S10. The fitted area ratio of peak I, II, and III in the range of 1720-1600 cm^{-1} corresponding to C=O stretching vibration.

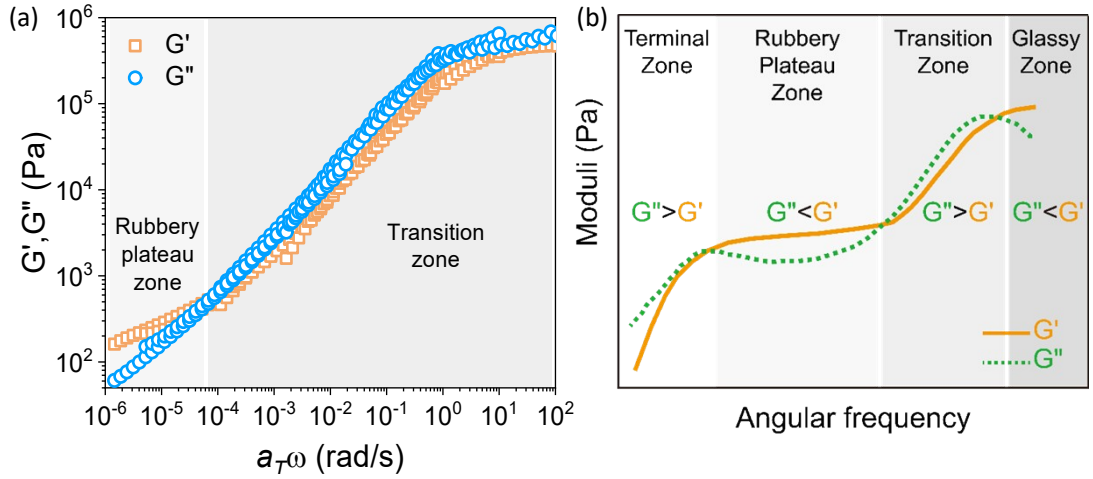

Figure S11. (a) The master curve of G′ and G″ for D230-0.9, the reference temperature is 25°C. (b) Illustration of the representative G′ and G″ master curves for typical viscoelastic polymer.

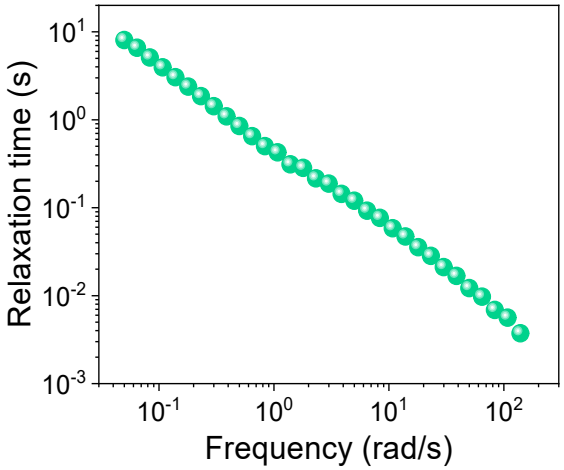

Figure S12. Relaxation time curves of the D230-0.9 (frequency range 0.05-100 rad s^{-1}, 25 °C). The segmental relaxation behavior was examined on the basis of the relaxation time obtained from the frequency-sweep data:

$$\frac{G'}{(|\eta^*|\omega)^2} = \frac{\tau}{|\eta^*|} \qquad \text{Equation S1}$$

where G', η^*, and τ are the storage modulus, complex viscosity, and relaxation time, respectively. The τ_s was obtained from the τ value at 0.05 rad/s.

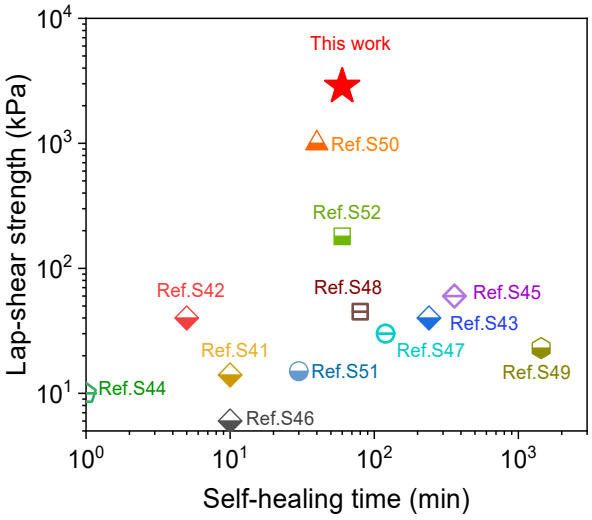

Figure S13. The comparison of the self-healing speed and adhesive strength between D230-0.9 and other reported adhesives.

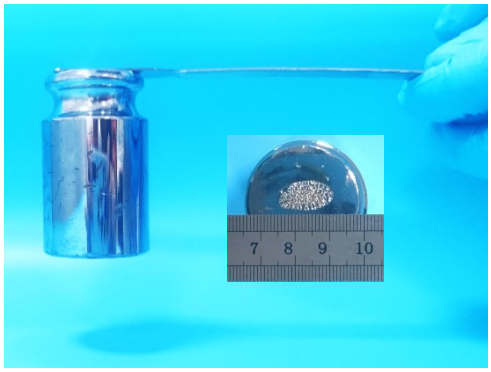

Figure S14. D230-0.9 could lift a weight of 500 g just by finger gently pressing with an adhesion area of 0.5 cm^2

Figure S15. The bonding process of PSA under gently pressing by dovetail clip.

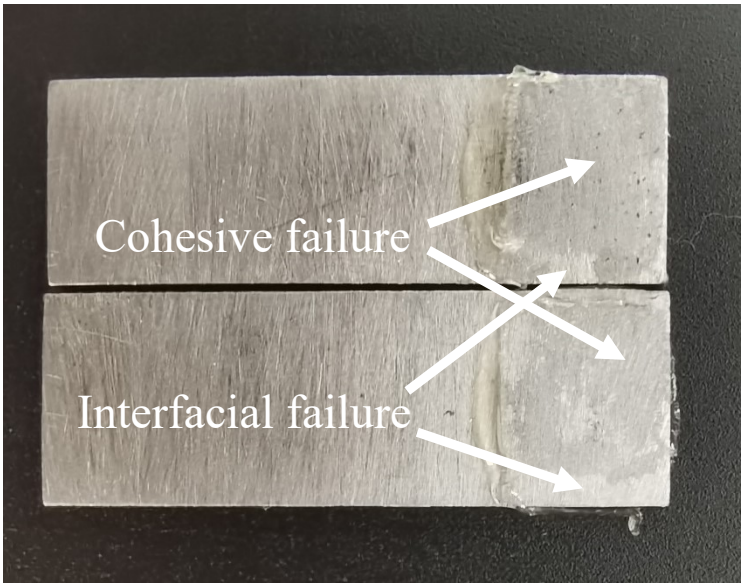

Figure S16. The fracture surface of D230-0.9 bonded to stainless steel as PSA.

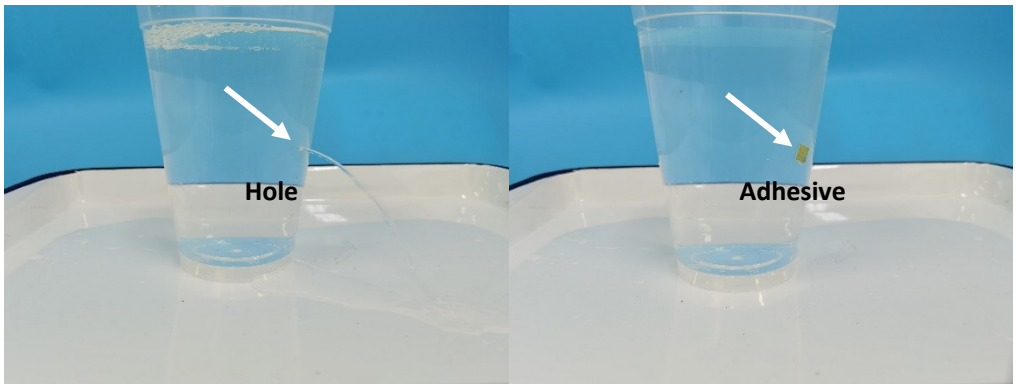

Figure S17. D230-0.9 as PSA could adhere the hole in polypropylene buckets to prevent further water leakage with bonded area of only 1cm^2.

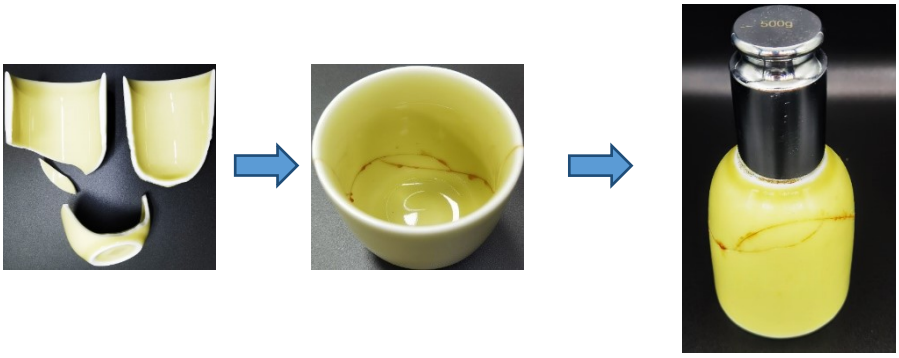

Figure S18. The D230-0.9 exhibits considerable bonding ability to ceramic, which allowing broken ceramic mugs to be restored by hand force alone.

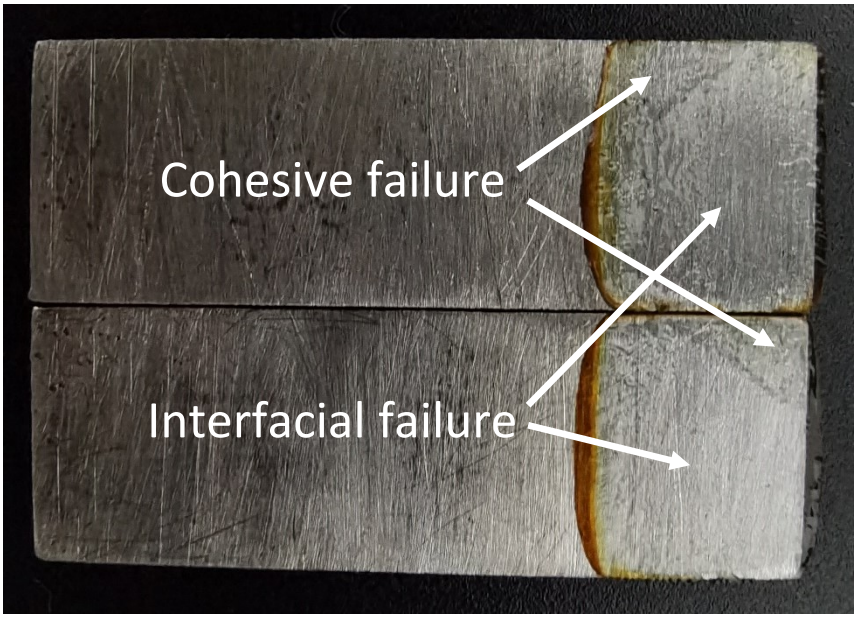

Figure S19. The fracture surface of D230-0.9 bonded to stainless steel as HMA.

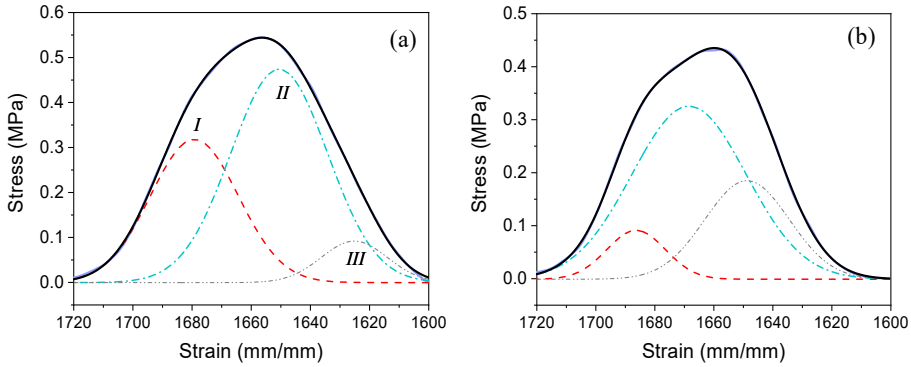

Figure S20. The FTIR spectrum and fitted curves at the range of 1720-1600 cm^{-1} corresponding to the stretching vibration of C=O band. (a) before heating; (b) after cooling.

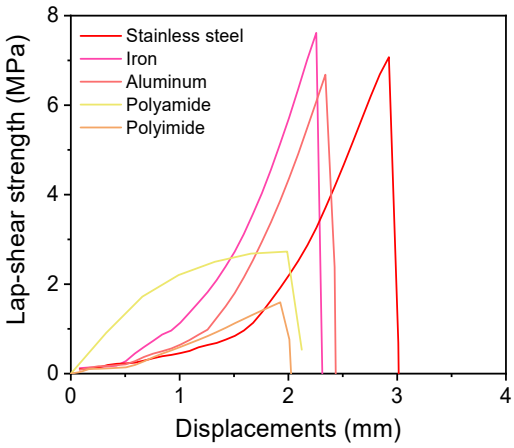

Figure S21. The lap-shear stress versus displacement of D230-0.9 as HMA bonded to the stainless steel, iron, aluminum, polyamide and polyimide, respectively.

Figure S22. The digital picture of D230-0.9 dissolved in ethanol.

Table S1. Summary of the assignment of the FTIR absorption bands for the hyperbranched polymers.

FTIR bands (cm^{-1})	Assignment (cm^{-1})
3380	ν(N-H) of primary amine ν(N-H)
3302	ν(N-H) of amide
3064	$\nu(NH_3^+)$
1719	ν(C=O)
1656	ν(N-H) of amide I
1536	ν(N-H) of amide II
1130	ν(C-F)
1050	ν(S-N-S)
987	δ(C=C)
950	δ(C=C)
760	Oxygen environment of $TFSI^-$ (bonded)[3]
739	Oxygen environment of $TFSI^-$ (free)[3]

Table S2. The carbon (C), oxygen (O), nitrogen (N), fluorine (F), sulfur (S) elements contents of D230-0.8, D230-0.9 and D230-1.0, respectively.

Elements	D230-0.8		D230-0.9		D230-1.0	
	Theoretical (%)	Experimental (%)	Theoretical (%)	Experimental (%)	Theoretical (%)	Experimental (%)
C	48.90	45.78	49.80	47.90	50.70	47.87
O	20.70	23.64	20.50	21.97	20.40	24.61
F	15.40	12.62	14.70	13.04	13.90	11.75
N	9.80	12.33	10.10	12.23	10.40	10.98
S	5.20	5.63	4.90	4.86	4.60	4.79

Table S3. The summary of mechanical properties of such hyperbranched polymers.

Samples	Young's Modulus (MPa)	Strength (MPa)	Enlongation at break (%)	Toughenss (kJ/m^3)
HDA-0.9	43.95	3.57	20	1215.87
D230-0.8	0.28	0.14	1685	949.67
D230-0.9	4.52	1.24	944	6525.42
D230-1.0	38.52	1.48	614	6673.85
D400-0.9	0.75	0.50	743	1714.46

Table S4. Summary of the assignment of the deconvoluted subpeaks in the FTIR C=O absorption bands for the D230-0.9.

Assignment		Wavenumber (cm^{-1})			
		D230-0.8	**D230-0.9**	**D230-1.0**	**D230-0.9 after cooling**
ν (C=O)	Free	1682	1680	1677	1679
	H-bonded (disorder)	1652	1650	1648	1650
	H-bonded (Order)	1616	1625	1627	1625
Total degree of H-bonds		75.5	77.9	81.4	90.7

The calculation process is expressed as:

The total content of H-bonds = $1-\frac{A_{Free}}{A_{total}}\times 100\%$

The content of order H-bonds = $\frac{A_{order}}{A_{total}}\times 100\%$

Table S5. Temperature-dependent storage modulus (*G'*) and loss modulus (*G''*) of D230-0.9 and reported polymers.

Supramolecular network polymers	Temperature (°C)	*G'* or *G''*	Reference
SHR	20 to 160	*G'* 20 MPa to 10 KPa *G''* 20 MPa to 1 KPa	[4]*Macromolecules* 2013, 46, 1841
Tr-PIB	-20 to 120	*G'* 3 MPa to 100 KPa *G''* 4 MPa to 2 KPa	[5]*Macromolecules* 2014, 47, 2122
polyurethane	0 to 120	*G'* 3 MPa to 40 Pa *G''* 0.5 MPa to 1 KPa	[6]*Chem. Sci.* 2016, 7, 4291
poly(TA-DIB-Fe)	25 to 120	*G'* 0.2 MPa to 7 KPa *G''* 0.1 MPa to 7 KPa	[7]*Sci. Adv.* 2018, 4, eaat8192
PDMS-Cat1-Zn	20 to 120	*G'* 10 MPa to 2 KPa *G''* 1 MPa to 10 KPa	[8]*ACS Appl. Mater. Interfaces* 2019, 11, 47382
DESPs	20 to 80	*G'* 10 MPa to 5 KPa *G''* 10 MPa to 3 KPa	[9]*Angew. Chem. Int. Ed.* 2020, 59, 11871
poly (TA)	20 to 100	*G'* 1 MPa to 100 Pa *G''* 1 MPa to 500 Pa	[10]*ACS Appl. Mater. Interfaces* 2021, 13, 44860
SEA-0.2	20 to 60	*G'* 0.1 GPa to 10 KPa *G''* 0.1 GPa to 10 KPa	[11]*ACS Mater. Lett.* 2021, 3, 1003
P(T0.7-co-A0.3)	60 to 130	*G'* 0.18 MPa to 4.8 KPa *G''* 0.12 MPa to 4.8 KPa	[12]*Adv. Funct. Mater.* 2022, 2112741
SMP0.9GNs0.1	20 to 120	*G'* 0.6 GPa to 2 MPa *G''* 0.2 GPa to 1 MPa	[13]*Chem. Eng. J.* 2022, 433, 133840
D230-0.9	25 to 150	*G'* 0.07 MPa to 1.1 Pa *G''* 0.12 MPa to 2.1 Pa	This work

Table S6. The self-healing efficiency of D230-0.9 at ambient temperature.

Self-healing time (min)	Strength (%)	Modulus (%)	Toughness (%)
10	44.0	90.7	25.6
30	75.4	89.3	52.5
60	92.7	92.0	91.3

The cited references in **Figure 3c**.

The comparison the lap-shear strength of D230-0.9 and other reported PSAs.[14-40]

The cited references in **Figure S13**.

The comparison of the self-healing speed and adhesive strength between D230-0.9 and other reported adhesives.[7, 24, 41-50]

Captions of videos:

Video S1. D230-0.9 bonded to three pieces of stainless steel under gently pressing could lift a dumbbell with weight of 10 kg.

Video S2. D230-0.9 as PSA could adhere the hole in polypropylene buckets to prevent further water leakage with bonded area of only 1cm^2.

Video S3. Pressing the sandwiched D230-0.9 as PSA between two pieces of conductive glass in a close circuit could light the bulbs up.

Video S4. Cyclic pressing-releasing of the sandwiched D230-0.9 as HMA between two pieces of conductive glass in a close circuit could change the brightness of bulbs.

References:

(1) Pérez, E.; Martínez, A.; Teijón, C.; Teijón, J. M.; Blanco, M. D. Bioresponsive nanohydrogels based on HEAA and NIPA for poorly soluble drugs delivery. *Int. J. Pharm.* **2014,** *470*, 107-19.

(2) Zhang, J.; Liang, X.; Zhang, Y.; Shang, Q. Fabrication and evaluation of a novel polymeric hydrogel of carboxymethyl chitosan-g-polyacrylic acid (CMC-g-PAA) for oral insulin delivery. *RSC. Adv.* **2016,** *6*, 52858-52867.

(3) Li, M.; Chen, L.; Li, Y.; Dai, X.; Jin, Z.; Zhang, Y.; Feng, W.; Yan, L.-T.; Cao, Y.; Wang, C. Superstretchable, yet stiff, fatigue-resistant ligament-like elastomers. *Nat. Commun.* **2022,** *13*, 2279

(4) Zhang, R.; Yan, T.; Lechner, B.-D.; Schröter, K.; Liang, Y.; Li, B.; Furtado, F.; Sun, P.; Saalwächter, K. Heterogeneity, Segmental and Hydrogen Bond Dynamics, and Aging of Supramolecular Self-Healing Rubber. *Macromolecules* **2013,** *46*, 1841-1850.

(5) Yan, T.; Schröter, K.; Herbst, F.; Binder, W. H.; Thurn-Albrecht, T. Nanostructure and Rheology of Hydrogen-Bonding Telechelic Polymers in the Melt: From Micellar Liquids and Solids to Supramolecular Gels. *Macromolecules* **2014,** *47*, 2122-2130.

(6) Feula, A.; Tang, X.; Giannakopoulos, I.; Chippindale, A. M.; Hamley, I. W.; Greco, F.; Paul Buckley, C.; Siviour, C. R.; Hayes, W. An adhesive elastomeric supramolecular polyurethane healable at body temperature. *Chem. Sci.* **2016,** *7*, 4291-4300.

(7) Zhang, Q.; Shi, C.-Y.; Qu, D.-H.; Long, Y.-T.; Feringa, B. L.; Tian, H. Exploring a naturally tailored small molecule for stretchable, self-healing, and adhesive supramolecular polymers. *Sci. Adv.* **2018,** *4*, eaat8192.

(8) Yi, B.; Liu, P.; Hou, C.; Cao, C.; Zhang, J.; Sun, H.; Yao, X. Dual-Cross-Linked Supramolecular Polysiloxanes for Mechanically Tunable, Damage-Healable and Oil-Repellent Polymeric Coatings. *ACS Appl. Mater. Inter.* **2019,** *11*, 47382-47389.

(9) Wu, S.; Cai, C.; Li, F.; Tan, Z.; Dong, S. Deep Eutectic Supramolecular Polymers: Bulk Supramolecular Materials. *Angew. Chem. Int. Edit.* **2020,** *59*, 11871-11875.

(10) Shi, C.-Y.; Zhang, Q.; Wang, B.-S.; Chen, M.; Qu, D.-H. Intrinsically Photopolymerizable Dynamic Polymers Derived from a Natural Small Molecule. *ACS Appl. Mater. Inter.* **2021,** *13*, 44860-44867.

(11) Sun, P.; Li, Y.; Qin, B.; Xu, J.-F.; Zhang, X. Super Strong and Multi-Reusable Supramolecular Epoxy Hot Melt Adhesives. *ACS Mater. Lett.* **2021,** *3*, 1003-1009,.

(12) Tian, Y.; Wu, J.; Fang, X.; Guan, L.; Yao, N.; Yang, G.; Wang, Z.; Hua, Z.; Liu, G. Rational Design of Bioinspired Nucleobase-Containing Polymers as Tough Bioplastics and Ultra-Strong Adhesives. *Adv. Funct. Mater.* **2022,** *32*, 2112741.

(13) Zhang, M.-H.; Li, C.-H.; Zuo, J.-L. A variable stiffness adhesive enabled by joule heating effect. *Chem. Eng. J.* **2022,** *433*, 133840.

(14) Cui, C.; Gu, R.; Wu, T.; Yuan, Z.; Fan, C.; Yao, Y.; Xu, Z.; Liu, B.; Huang, J.; Liu, W. Zwitterion-Initiated Spontaneously Polymerized Super Adhesive Showing Real-Time Deployable and Long-Term High-Strength Adhesion against Various Harsh Environments. *Adv. Funct. Mater.* **2022,** *32*, 2109144.

(15) Hao, S.; Li, T.; Yang, X.; Song, H. Ultrastretchable, Adhesive, Fast Self-Healable, and Three-Dimensional Printable Photoluminescent Ionic Skin Based on Hybrid Network Ionogels. *ACS Appl. Mater. Inter.* **2022,** *14*, 2029-2037.

(16) Yu, Z.; Wu, P. Underwater Communication and Optical Camouflage Ionogels. *Adv. Mater.* **2021,** *33*, 2008479.

(17) Zhu, J.; Lu, X.; Zhang, W.; Liu, X. Substrate-Independent, Reversible, and Easy-Release Ionogel Adhesives with High Bonding Strength. *Macromol. Rapid. Comm.* **2020,** *41*, 2000098.

(18) Kato, R.; Mirmira, P.; Sookezian, A.; Grocke, G. L.; Patel, S. N.; Rowan, S. J. Ion-Conducting Dynamic Solid Polymer Electrolyte Adhesives. *ACS Macro. Lett.* **2020,** *9*, 500-506.
(19) Yu, Z.; Wu, P. Water-Resistant Ionogel Electrode with Tailorable Mechanical Properties for Aquatic Ambulatory Physiological Signal Monitoring. *Adv. Funct. Mater.* **2021,** *31*, 2107226.
(20) Zhao, L.; Wang, B.; Mao, Z.; Sui, X.; Feng, X. Nonvolatile, stretchable and adhesive ionogel fiber sensor designed for extreme environments. *Chem. Eng. J.* **2022,** *433*, 133500.
(21) Sun, J.; Yuan, Y.; Lu, G.; Li, L.; Zhu, X.; Nie, J. A transparent, stretchable, stable, self-adhesive ionogel-based strain sensor for human motion monitoring. *J. Mater. Chem. C.* **2019,** *7*, 11244-11250.
(22) Xu, J.; Guo, Z.; Chen, Y.; Luo, Y.; Xie, S.; Zhang, Y.; Tan, H.; Xu, L.; Zheng, J. Tough, adhesive, self-healing, fully physical crosslinked κ-CG-K+/pHEAA double-network ionic conductive hydrogels for wearable sensors. *Polymer* **2021,** *236*, 124321.
(23) Mo, J.; Dai, Y.; Zhang, C.; Zhou, Y.; Li, W.; Song, Y.; Wu, C.; Wang, Z. Design of ultra-stretchable, highly adhesive and self-healable hydrogels via tannic acid-enabled dynamic interactions. *Mater. Horiz.* **2021,** *8*, 3409-3416.
(24) Gao, G.; Yang, F.; Zhou, F.; He, J.; Lu, W.; Xiao, P.; Yan, H.; Pan, C.; Chen, T.; Wang, Z. L. Bioinspired Self-Healing Human–Machine Interactive Touch Pad with Pressure-Sensitive Adhesiveness on Targeted Substrates. *Adv. Mater.* **2020,** *32*, 2004290.
(25) Fu, Q.; Hao, S.; Meng, L.; Xu, F.; Yang, J. Engineering Self-Adhesive Polyzwitterionic Hydrogel Electrolytes for Flexible Zinc-Ion Hybrid Capacitors with Superior Low-Temperature Adaptability. *ACS nano* **2021,** *15*, 18469-18482.
(26) Zhou, H.; Lai, J.; Jin, X.; Liu, H.; Li, X.; Chen, W.; Ma, A.; Zhou, X. Intrinsically adhesive, highly sensitive and temperature tolerant flexible sensors based on double network organohydrogels. *Chem. Eng. J.* **2021,** *413*, 127544.
(27) Fang, K.; Gu, Q.; Zeng, M.; Huang, Z.; Qiu, H.; Miao, J.; Fang, Y.; Zhao, Y.; Xiao, Y.; Xu, T.; Golodok, R. P.; Savich, V. V.; Ilyushchenko, A. P.; Ai, F.; Liu, D.; Wang, R. Tannic acid-reinforced zwitterionic hydrogels with multi-functionalities for diabetic wound treatment. *J. Mater. Chem. B.* **2022,** *10*, 4142-4152.
(28) Bai, J.; Wang, R.; Wang, X.; Liu, S.; Wang, X.; Ma, J.; Qin, Z.; Jiao, T. Biomineral calcium-ion-mediated conductive hydrogels with high stretchability and self-adhesiveness for sensitive iontronic sensors. *Cell Reports Physical Science* **2021,** *2*, 100623.
(29) Qu, X.; Wang, S.; Zhao, Y.; Huang, H.; Wang, Q.; Shao, J.; Wang, W.; Dong, X. Skin-inspired highly stretchable, tough and adhesive hydrogels for tissue-attached sensor. *Chem. Eng. J.* **2021,** *425*, 131523.
(30) Pei, D.; Yu, S.; Zhang, X.; Chen, Y.; Li, M.; Li, C. Zwitterionic dynamic elastomer with high ionic conductivity for self-adhesive and transparent electronic skin. *Chem. Eng. J.* **2022,** *445*, 136741.
(31) Cui, C.; Fan, C.; Wu, Y.; Xiao, M.; Wu, T.; Zhang, D.; Chen, X.; Liu, B.; Xu, Z.; Qu, B.; Liu, W. Water-Triggered Hyperbranched Polymer Universal Adhesives: From Strong Underwater Adhesion to Rapid Sealing Hemostasis. *Adv. Mater.* **2019,** *31*, 1905761.
(32) Zheng, S. Y.; Zhou, J.; Wang, S.; Wang, Y.-J.; Liu, S.; Du, G.; Zhang, D.; Fu, J.; Lin, J.; Wu, Z. L.; Zheng, Q.; Yang, J. Water-Triggered Spontaneously Solidified Adhesive: From Instant and Strong Underwater Adhesion to In Situ Signal Transmission. *Adv. Funct. Mater* ***2022,*** 32, 2205597.
(33) Moon, H.; Jeong, K.; Kwak, M. J.; Choi, S. Q.; Im, S. G. Solvent-Free Deposition of Ultrathin Copolymer Films with Tunable Viscoelasticity for Application to Pressure-Sensitive Adhesives. *ACS Appl. Mater. Inter.* **2018,** *10*, 32668-32677.

(34) Niu, W.; Zhu, J.; Zhang, W.; Liu, X. Simply Formulated Dry Pressure-Sensitive Adhesives for Substrate-Independent Underwater Adhesion. *ACS Mater. Lett.* **2022,** *4*, 410-417.
(35) Fan, H.; Wang, J.; Tao, Z.; Huang, J.; Rao, P.; Kurokawa, T.; Gong, J. P. Adjacent cationic–aromatic sequences yield strong electrostatic adhesion of hydrogels in seawater. *Nat. Commun.* **2019,** *10*, 5127.
(36) Yi, H.; Lee, S.-H.; Ko, H.; Lee, D.; Bae, W.-G.; Kim, T.-i.; Hwang, D. S.; Jeong, H. E. Ultra-Adaptable and Wearable Photonic Skin Based on a Shape-Memory, Responsive Cellulose Derivative. *Adv. Funct. Mater.* **2019,** *29*, 1902720.
(37) Yu, X.; Zheng, Y.; Zhang, H.; Wang, Y.; Fan, X.; Liu, T. Fast-Recoverable, Self-Healable, and Adhesive Nanocomposite Hydrogel Consisting of Hybrid Nanoparticles for Ultrasensitive Strain and Pressure Sensing. *Chem. Mater.* **2021,** *33*, 6146-6157.
(38) Chun, S.; Kim, D. W.; Baik, S.; Lee, H. J.; Lee, J. H.; Bhang, S. H.; Pang, C. Conductive and Stretchable Adhesive Electronics with Miniaturized Octopus-Like Suckers against Dry/Wet Skin for Biosignal Monitoring. *Adv. Funct. Mater.* **2018,** *28*, 1805224.
(39) He, Y.; Deng, Z.; Wang, Y.-J.; Zhao, Y.; Chen, L. Polysaccharide/Ti3C2Tx MXene adhesive hydrogels with self-healing ability for multifunctional and sensitive sensors. *Carbohyd. Polym.* **2022,** *291*, 119572.
(40) He, Z.; Yuan, W. Highly Stretchable, Adhesive Ionic Liquid-Containing Nanocomposite Hydrogel for Self-Powered Multifunctional Strain Sensors with Temperature Tolerance. *ACS Appli. Mater. Inter.* **2021,** *13*, 53055-53066.
(41) He, J.; Zhang, Z.; Yang, Y.; Ren, F.; Li, J.; Zhu, S.; Ma, F.; Wu, R.; Lv, Y.; He, G.; Guo, B.; Chu, D. Injectable Self-Healing Adhesive pH-Responsive Hydrogels Accelerate Gastric Hemostasis and Wound Healing. *Nano-Micro Letters* **2021,** *13*, 80.
(42) Gao, G.; Yang, F.; Zhou, F.; He, J.; Lu, W.; Xiao, P.; Yan, H.; Pan, C.; Chen, T.; Wang, Z. L. Bioinspired Self-Healing Human–Machine Interactive Touch Pad with Pressure-Sensitive Adhesiveness on Targeted Substrates. *Adv. Mater.* **2020,** *32*, 2004290.
(43) Zhang, L. M.; He, Y.; Cheng, S.; Sheng, H.; Dai, K.; Zheng, W. J.; Wang, M. X.; Chen, Z. S.; Chen, Y. M.; Suo, Z. Self-Healing, Adhesive, and Highly Stretchable Ionogel as a Strain Sensor for Extremely Large Deformation. *Small* **2019,** *15*, 1804651.
(44) Zheng, H.; Lin, N.; He, Y.; Zuo, B. Self-Healing, Self-Adhesive Silk Fibroin Conductive Hydrogel as a Flexible Strain Sensor. *ACS Appli. Mater. Inter.* **2021,** *13*, 40013-40031.
(45) Xu, Z.; Chen, L.; Lu, L.; Du, R.; Ma, W.; Cai, Y.; An, X.; Wu, H.; Luo, Q.; Xu, Q.; Zhang, Q.; Jia, X. A Highly-Adhesive and Self-Healing Elastomer for Bio-Interfacial Electrode. *Adv. Funct. Mater.* **2021,** *31*, 2006432.
(46) Zhao, L.; Ren, Z.; Liu, X.; Ling, Q.; Li, Z.; Gu, H. A Multifunctional, Self-Healing, Self-Adhesive, and Conductive Sodium Alginate/Poly(vinyl alcohol) Composite Hydrogel as a Flexible Strain Sensor. *ACS Appli. Mater. Inter.* **2021,** *13*, 11344-11355.
(47) Zhou, L.; Dai, C.; Fan, L.; Jiang, Y.; Liu, C.; Zhou, Z.; Guan, P.; Tian, Y.; Xing, J.; Li, X.; Luo, Y.; Yu, P.; Ning, C.; Tan, G. Injectable Self-Healing Natural Biopolymer-Based Hydrogel Adhesive with Thermoresponsive Reversible Adhesion for Minimally Invasive Surgery. *Adv. Funct. Mater.* **2021,** *31*, 2007457.
(48) Qiao, H.; Qi, P.; Zhang, X.; Wang, L.; Tan, Y.; Luan, Z.; Xia, Y.; Li, Y.; Sui, K. Multiple Weak H-Bonds Lead to Highly Sensitive, Stretchable, Self-Adhesive, and Self-Healing Ionic Sensors. *ACS Appli. Mater. Inter.* **2019,** *11*, 7755-7763.
(49) Pei, X.; Zhang, H.; Zhou, Y.; Zhou, L.; Fu, J. Stretchable, self-healing and tissue-adhesive

zwitterionic hydrogels as strain sensors for wireless monitoring of organ motions. *Mater. Horiz.* **2020,** *7*, 1872-1882.
(50) Zhang, Q.; Shi, C.-Y.; Qu, D.-H.; Long, Y.-T.; Feringa, B. L.; Tian, H. Exploring a naturally tailored small molecule for stretchable, self-healing, and adhesive supramolecular polymers. *Sci. Adv.* **2018,** *4*, eaat8192.
(51) Shao, C.; Wang, M.; Meng, L.; Chang, H.; Wang, B.; Xu, F.; Yang, J.; Wan, P. Mussel-Inspired Cellulose Nanocomposite Tough Hydrogels with Synergistic Self-Healing, Adhesive, and Strain-Sensitive Properties. *Chem. Mater.* **2018,** *30*, 3110-3121.
(52) Liang, Y.; Xu, H.; Li, Z.; Zhangji, A.; Guo, B. Bioinspired Injectable Self-Healing Hydrogel Sealant with Fault-Tolerant and Repeated Thermo-Responsive Adhesion for Sutureless Post-Wound-Closure and Wound Healing. *Nano-Micro Letters* **2022,** *14*, 185.